



The Effects of Attractive Interaction on Viscosity in Undercooled Kob–Andersen Liquids

Vichhika Moul¹ · Younggak Shin¹ · Byeongchan Lee¹

Received: 6 November 2023 / Revised: 30 November 2023 / Accepted: 2 December 2023 / Published online: 17 February 2024
© The Author(s) under exclusive licence to Korea Multi-Scale Mechanics (KMSM) 2024

Abstract

We present the effects of interatomic attraction on liquid fragility from atomistic calculations. Shear viscosity is sensitive to thermodynamic conditions as well as numerical setups, and deeper undercooling substantially increases the viscosity of the Kob–Andersen liquids due to the reduced atomic mobility. The attractive force plays a major role in determining the viscosity and liquid fragility in the undercooled region, and the viscosity in the presence of attractive interactions more rapidly increases as the temperature drops, showing a super-Arrhenius behavior of a fragile liquid. On the contrary, a liquid of purely repulsive atoms is found to be a strong liquid. The computational cost nearly doubles for the undercooled liquids along with the attractive interaction as the correlation of dynamic properties persists longer due to higher viscosity.

Keywords System size effect · Attractive force effect · Shear viscosity · Liquid fragility · Undercooled liquids

Introduction

The dynamic properties of undercooled liquids are of particular interest as they are key to understanding glass-forming ability [1]. The dynamic properties of glass-forming liquids are found to be sensitive to the change in state variables such as temperature and pressure, and the shear viscosity in particular may vary over orders of magnitude in undercooled liquids as temperature is decreased from the melting to the glass transition temperature [2]. The liquid fragility of a glass-former quantifies how rapidly viscosity changes upon undercooling. The fragile liquids with a rapid change in viscosity shows a super-Arrhenius behavior which can be differentiated from an Arrhenius-type response of strong liquids [3].

To understand various properties of undercooled liquids, molecular dynamics (MD) has been extensively used as atomic as well as electronic information is directly accessible [4, 5], and the Kob–Andersen (KA) [6] model is often used because it does not form a crystalline phase. The KA model simplifies the interatomic interactions but still bears

the physical relevance as shown in the Ni₈₀P₂₀ alloy [7]. Model materials are often used to study specific behaviors of liquids, and give insights on material properties of liquids such as fragility and heterogeneity [8].

In classical MD studies, the role of attractive and repulsive interactions in liquids have been also studied [1, 9–11]. An 8:2 binary mixture within the Lennard–Jones potential (KA–LJ) is known to be a good glass former in the three-dimensional space, but the glass-forming ability (GFA) is sensitive to the composition, binding energies, and environment. For example, a different binary mixture such as 6.5:3.5 may show the highest GFA in the two dimensional space but not necessarily in the three dimensional space [12]. In the KA–LJ model, the binding energy between different elements is substantially larger than the binding between like atoms whereas the difference between the atomic radii is as much as 20 percent, preventing crystallization [13]. The KA–LJ liquid at density of 1.2 is reported to have the melting temperature of 1.028 at the corresponding pressure of 10.19 in reduced units [14], and known to be fragile [2, 15]. The glass-transition temperature in metals is the temperature above which a solid yet amorphous structure is energetically more stable than the crystalline phase. For KA, the glass-transition temperature is 0.41 in reduced units [16], and the glass-transition temperature and the fragility of liquid are correlated to GFA.

✉ Byeongchan Lee
airbc@khu.ac.kr

¹ Department of Mechanical Engineering, Kyung Hee University, 1732 Deogyong-daero, Yongin, Gyeonggi 17104, Republic of Korea

To better understand the effects of attractive and repulsive interatomic interactions on structural and dynamic properties of glassy systems, the reduction to purely repulsive part of the pair potential Weeks–Chandler–Andersen (WCA) [17] variants of KA–LJ have been studied [9, 18]. Liquid structures found with both interatomic potentials are almost identical, but the structural relaxation time differs by orders of magnitude. Nevertheless, the comparison between KA–LJ and KA–WCA has yet to be done for a better understanding on the viscosity and hence liquid fragility.

The temperature dependence of viscosity in KA model at constant pressure was studied by Mukherjee [2]. It is reported that KA model shows a super-Arrhenius dependence of viscosity, although there was no detail information on the effect of pair potential on viscosity given. To investigate the pair potential effect on viscosity and the cause of super-Arrhenius behavior in KA model, we examine the temperature dependence of viscosity in larger systems at constant density of two KA models, with and without attractive interaction. We found different behaviors between the two models when cooling toward glass-transition temperature showing different liquid fragility, showing different GFA.

Here we present our calculation results on viscosity over wide range of temperature using both KA–LJ and KA–WCA models. To ensure the convergence of viscosity and to confirm the size dependence, we also study the effects of system size on viscosity. “Materials and methods” refers to materials and methods that are used to simulate the systems and calculate the viscosity. The calculation results for system size and pair potential effects on fragility are presented and discussed in “Results and discussions”. “Conclusions” is the conclusions.

Materials and Methods

Kob–Andersen Binary Mixture of Lennard–Jones

The KA model is based on the Lennard–Jones (LJ) potential [19], and defined as

$$u_{ij}^{LJ}(r) = \begin{cases} 4\epsilon_{ij}[(\frac{\sigma_{ij}}{r})^{12} - (\frac{\sigma_{ij}}{r})^6], & \text{if } r < r_c^{LJ} \\ 0, & \text{otherwise} \end{cases} \quad (1)$$

where indices $i, j = A, B$ represent different elements with element A larger than element B in terms of atomic radius. The list of parameters used for the binary KA–LJ potentials are as follows; $\sigma_{AA} = 1.0, \sigma_{BB} = 0.88\sigma_{AA}, \sigma_{AB} = 0.8\sigma_{AA}, \epsilon_{AA} = 1.0, \epsilon_{BB} = 0.5\epsilon_{AA},$ and $\epsilon_{AB} = 1.5\epsilon_{AA}$. The chemical composition and mass ratios are 8:2 and 1:1 respectively. The cutoff radius is assumed to be $r_c^{LJ} = 2.5\sigma_{ij}$, and hence depends on elements.

The reduction to the purely repulsive pair potential, KA–WCA, is described as

$$u_{ij}^{WCA}(r) = \begin{cases} 4\epsilon_{ij}[(\frac{\sigma_{ij}}{r})^{12} - (\frac{\sigma_{ij}}{r})^6 + C_{ij}], & \text{if } r < r_c^{WCA} \\ 0, & \text{otherwise} \end{cases} \quad (2)$$

The KA–WCA potential parameters are identical to those of KA–LJ with an additional offset parameter C_{ij} . The whole KA–LJ energy curve is shifted by C_{ij} and truncated at r_c^{WCA} such that the interatomic repulsive force is preserved but the attractive interaction is eliminated. The cutoff and the offset are determined at the minimum u_{ij} of KA–LJ, i.e. $r_c^{WCA} = 2^{1/6} \sigma_{ij}$ but $C_{ij} = 1/4$ regardless of elements. The two models are compared in Fig. 1.

Green–Kubo Relation (GK)

The Green–Kubo (GK) relation [20] is used to predict the shear viscosity as a function of temperature within equilibrium molecular dynamics. The viscosity of undercooled liquids are reported to depend strongly on temperature [2], weakly on pressure [21], but not on system size [22, 23].

The GK relation can be used to calculate the shear viscosity η and described as

$$\eta = \frac{V}{k_B T} \sum_{\alpha \neq \beta} \eta_{\alpha\beta} \quad (3)$$

$$\eta_{\alpha\beta} = \frac{V}{k_B T} \int_0^\infty \langle \sigma_{\alpha\beta}(0) \sigma_{\alpha\beta}(t) \rangle dt \quad (4)$$

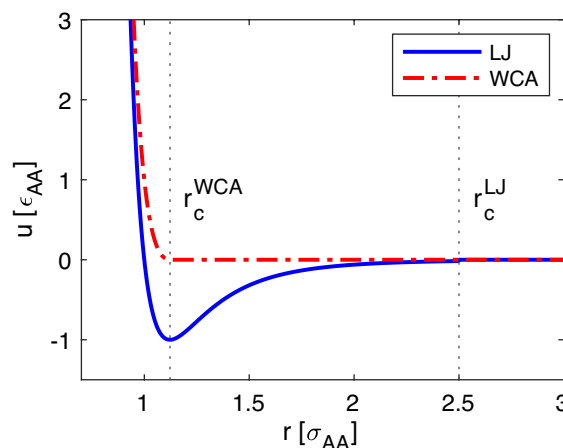


Fig. 1 Pair potential comparison. WCA reproduces the repulsive force of LJ as well as the potential energy relative to the minimum energy for $r < r_c^{WCA}$

$$\sigma_{\alpha\beta} V = \sum_{k=1}^N m_k v_{k\alpha} v_{k\beta} + \sum_{k=1}^N r_{k\alpha} f_{k\beta} \tag{5}$$

where $\sigma_{\alpha\beta}$ are the off-diagonal components of the stress tensor, and $\langle \sigma_{\alpha\beta}(0)\sigma_{\alpha\beta}(t) \rangle$ is an ensemble average of the stress autocorrelation function. $m_k, v_{k\alpha}, r_{k\alpha}, f_{k\beta}$ are mass, coordinate, velocity of the k th particle, and the force acting on the k th particle, respectively, in α, β -components. η^* is reduced viscosity where $\eta^* = \eta \frac{\sigma^3}{\epsilon \tau}$.

Simulation Detail

The Large-scale Atomic/Molecular Massively Parallel Simulator (LAMMPS) [24] is used for atomistic calculations, and the initial configurations are created with randomly distributed atoms in cubic periodic boxes from $N = 125$ to $N = 8000$ particles at the density of 1.2 in reduced units [14]. The time step is set to 0.001.

The system is relaxed at the initial temperature $T_i = 5.0$ to completely break potential orders, and then quenched to an individual target temperature T_f from 0.6 to 2.0. The system is further relaxed at T_f within the NPT ensemble 1 to 3×10^6 time steps to obtain the equilibrium volume, and finally equilibrated using GK for $10\text{--}30 \times 10^6$ time steps to obtain the statistics at a target temperature within the NVT ensemble using the Nose–Hoover thermostat. The dynamic properties are predicted from the final 30×10^3 steps equivalent to $\Delta\tau = 30$.

For shear viscosity calculation, stress autocorrelation functions (ACFs) are obtained from three off-diagonal components of stress tensor which are $\sigma_{xy}, \sigma_{xz}, \sigma_{yz}$. The viscosity η is calculated from an average over $\eta_{xy}, \eta_{xz}, \eta_{yz}$ as implemented in LAMMPS. The number of time stamps used to calculation correlation for given delay time varies from 10,000 to 50,000 steps depending on the temperature. The ACFs are further calculated using MATLAB [25] to analyze the change of ACF, integral, and viscosity curve at each temperature.

Results and Discussions

The system size effects on ACFs, integral of ACFs, and viscosity results are examined at temperature $T = 0.7$ for KA–LJ. The viscosity as a function of temperature from $T = 0.6\text{--}2.0$ are predicted and compared for 1000-atom KA–LJ and KA–WCA to observe the effect of repulsive interactions on viscosity and liquid fragility.

Decay Time of Autocorrelation Function

The ACF curves as a function of correlation time and system size at temperature $T = 0.7$ for KA–LJ are shown in Fig. 2a. The ACFs of the larger systems decay faster due to the size of the statistics: the atomic motions become seemingly less

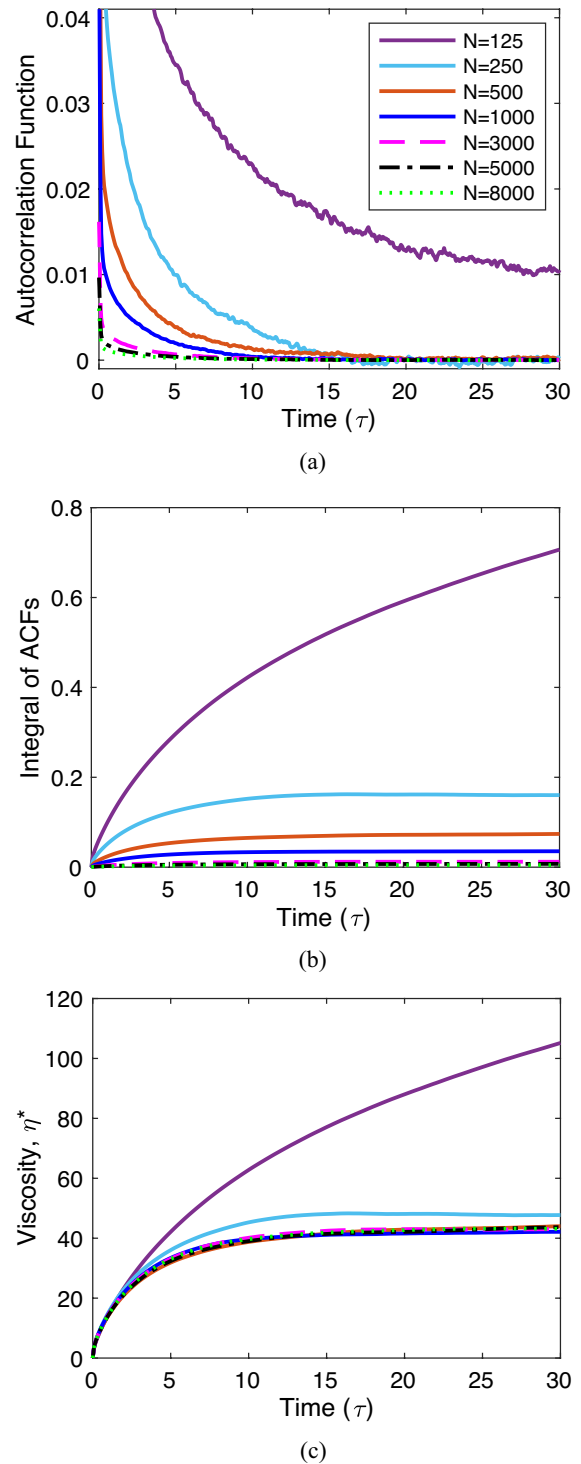


Fig. 2 Stress autocorrelation function (ACF) and its integral as a function of correlation time and system size for KA–LJ at $T=0.7$. **a** ACF, **b** integral of ACF, **c** viscosity (the ACF y-axis is zoomed in to illustrate the decay time)

correlated with the system size increased. The fluctuation in the curve is also reduced for bigger systems due to the same reason, confirming better statistics. On the same token, the

slow decay with large fluctuation make it difficult for small system to get dynamic properties accurately.

Integral of Autocorrelation Function

The integral in Eq. (4) is obtained from the ACF shown in Fig. 2a. Figure 2b illustrates the integral of ACFs, in which the size dependence is obvious as defined in Eq. (5). The plateau value represents the amount of correlation, and hence the system size. Notice that the smallest system with $N = 125$ does not reach the convergence for the maximum simulation time tested.

Shear Viscosity

The integral ACFs are normalized by volume and temperature as in Eq. (4) to predict the viscosity. The viscosity prediction during the simulation is also shown in Fig. 2c. The viscosity shows convergence against the system size when the simulation is run for very long enough, with no significant change beyond $N = 500$. This effect is expected from the slow decay in ACFs that leads to the difficulty in obtaining the reliable value of viscosity for $N < 500$.

Liquid Fragility

To ensure accuracy, the temperature dependence of viscosity is predicted with the system size of $N=1000$ for KA–LJ and KA–WCA models as shown in Fig. 3a. Regardless of model, the viscosity increases when temperature is decreased, but the change is dramatic for KA–LJ. The viscosity is nearly identical at $T = 2.0$, and remains comparable above melting temperature ($T = 1.028$). The viscosity of KA–LJ sharply increases from $T = 0.8$ to $T = 0.6$ as the system is undercooled towards the glass-transition temperature, whereas the viscosity of KA–WCA at $T = 0.6$ is only around 20 % of that of KA–LJ. This confirms that the attractive interactions play a critical role in the change of viscosity when temperature is changed in the undercooled regime.

The logarithm of viscosity against inverse temperature is plotted in Fig. 3b. KA–LJ exhibits super-Arrhenius dependence of viscosity, indicating a behavior of fragile liquid. The same behavior was reported for KA–LJ in previous study [2], yet [15] found that the fragility of KA is weak. This is consistent with our result in the plot as the dependence shows less deviated from the connected line. On the other hand, its purely repulsive force model KA–WCA shows a nearly linear and steady increase in viscosity. This increase displays Arrhenius dependence, which is considered as a strong liquid. The different Arrhenius dependences between KA–LJ and KA–WCA prove that the attraction plays a major role in determining the fragility of undercooled liquids.

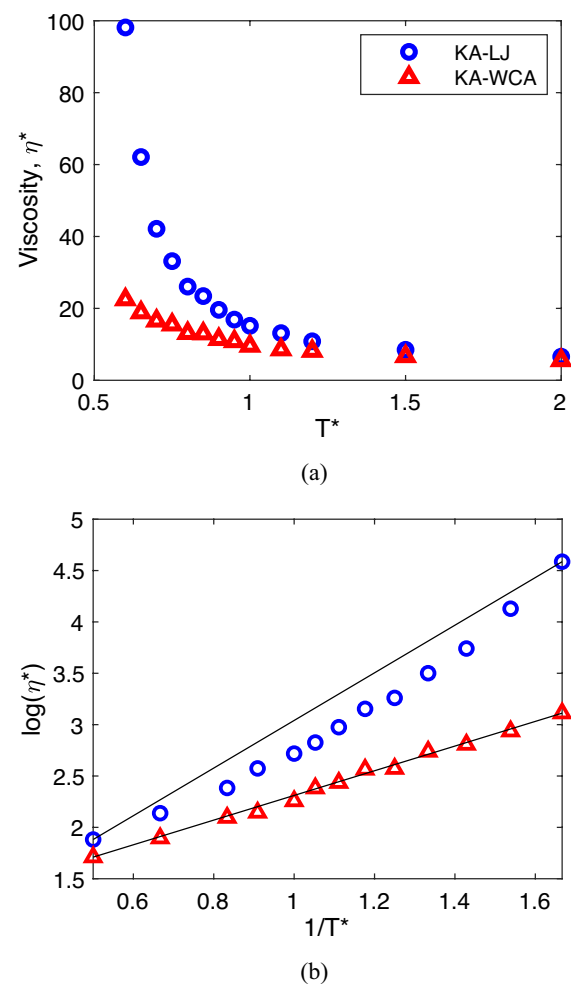


Fig. 3 The viscosity of KA–LJ and KA–WCA models with $N = 1000$, **a** viscosity as a function of temperature and **b** logarithm of viscosity as a function of inverse temperature. The solid lines connect the lower and the upper bounds to give a guide to eyes for fragility

Effects of Numerical Setup

Numerical setups beyond system size inevitably affects viscosity predictions, and here we discuss the effects of numerical setup on viscosity and fragility.

Sampling Rate

The shear stress is read off with two different sampling rates and compared for KA–LJ and KA–WCA in Fig. 4. A lower sampling rate results in the residual fluctuation in the ACF, and consequently the integral of ACF is hardly converged even for a longer period of simulation time as shown in Fig. 4a. The long trailing fluctuation of the calculated viscosity is indicative of the numerical instability. It can be empirical to find the threshold sampling rate, and we recommend that the stress sampling rate be set to be equal

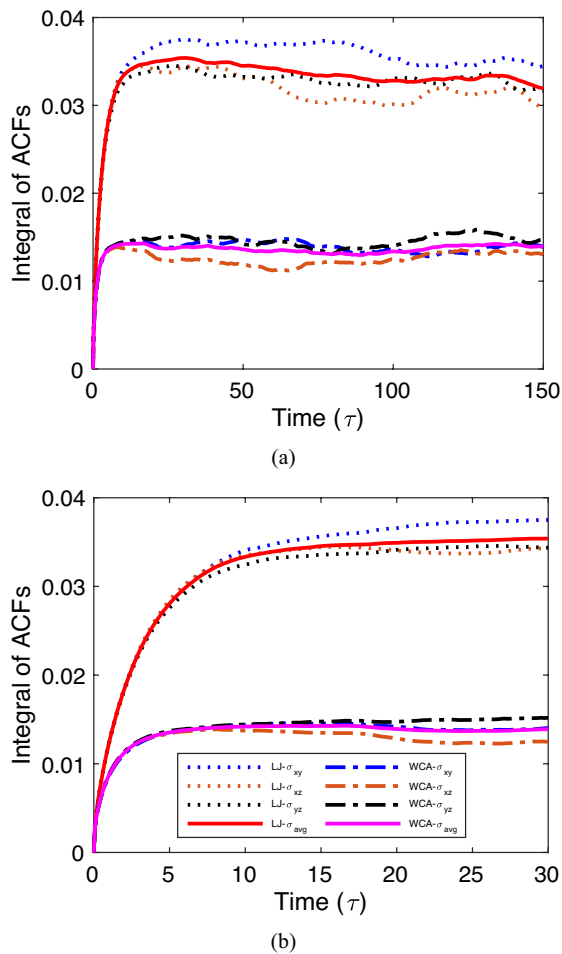


Fig. 4 The integrated ACFs for KA-LJ and KA-WCA with $N = 1000$. The 3 off-diagonal components of stress tensor and the average are calculated with the sampling rate of **a** every 5 steps, and **b** every step

to the time step. The 3 off-diagonal stress components are not identical, and a typical system size to guarantee the isotropy in mechanical properties of amorphous systems is at least an order of magnitude larger than the systems tested in this study [26]. Nevertheless, the convergence of viscosity against system size is suggestive of isotropy obtained for the averaged stress.

Calculation Temperature

ACF decays slowly when deeply undercooled as dynamics is slowed down below melting, and hence, calculating viscosity takes longer and more expensive in terms of calculation cost. The viscosity shown in Fig. 3 has been obtained with different time intervals, i.e. a longer period of time at lower temperature until the integral of ACF is converged. The integral and viscosity values increase with decreasing temperature.

Simulation Time

The system size effect commonly appears when the simulation time is too short to produce sufficient statistics, and the resulting properties will be inaccurate in a quantitative sense. The size effect can be reduced to some extent when the simulation lasts long enough to produce the statistics that would otherwise be generated with a bigger cell, e.g. at least 20×10^6 time steps at this studied temperature $T = 0.7$ for both KA-LJ and KA-WCA. Nevertheless, it is always better to increase the system size to obtain more accurate dynamic properties as correlations functions will be numerically more stable when the system size is bigger, e.g. non-decaying autocorrelation functions when N is too small.

The deeper undercooling in the presence of attractive interactions usually takes almost twice longer time to predict dynamic properties as the correlation persists longer. This is because both undercooling and attractive interactions increase viscosity, which requires more time for correlation functions to vanish.

Conclusions

In conclusion, we have found that attractive interaction substantially increases the viscosity of undercooled liquids of the KA binary model materials. The purely repulsive KA-WCA shows an Arrhenius behavior of viscosity, indicating a strong liquid. Above melting, adding attractive interactions to the model, i.e. KA-LJ, hardly changes the viscosity. We think this is because repulsive interactions in general predominantly determine structural and dynamics properties in the liquid phase.

The attractive interaction plays an increasingly important role in the shear viscosity and fragility when temperature is decreased below melting. The viscosity of KA-LJ rapidly increases, showing super-Arrhenius behavior of fragile liquids. The contribution of attractive interactions to the total viscosity near the glass-transition temperature is around 80%, changing GFA. The attractive contribution is critical in understanding dynamic properties of undercooled liquids, and hence LJ is more suitable to study undercooled liquids than WCA. Further improvements include the prediction of energetic and structural properties such as glass-transition temperature and pair-correlation function in the undercooled state, and a parametric study on the relative strength of the attractive interaction may shed lights on understanding liquid fragility.

Acknowledgements This research was supported by National R & D Program through the National Research Foundation of Korea (NRF) funded by the Ministry of Science & ICT (2020R1A2C201510914).

Data availability The authors declare that the data supporting the findings of this study can be made available upon reasonable request.

Declarations

Conflict of interest The authors have no conflicts of interest to declare that are relevant to the content of this article.

References

1. A. Singh, Y. Singh, How attractive and repulsive interactions affect structure ordering and dynamics of glass-forming liquids. *Phys. Rev. E* **103**(5), 052105 (2021)
2. A. Mukherjee, S. Bhattacharyya, B. Bagchi, Pressure and temperature dependence of viscosity and diffusion coefficients of a glassy binary mixture. *J. Chem. Phys.* **116**(11), 4577–4586 (2002)
3. C.A. Angell, Formation of glasses from liquids and biopolymers. *Science* **267**(5206), 1924–35 (1995)
4. B. Lee, G.W. Lee, Local structure of liquid Ti: ab initio molecular dynamics study. *J. Chem. Phys.* **129**(2), 024711 (2008)
5. G.W. Lee, Y.C. Cho, B. Lee, K.F. Kelton, Interfacial free energy and medium range order: proof of an inverse of Frank's hypothesis. *Phys. Rev. B* **95**(5), 054202 (2017)
6. W. Kob, H.C. Andersen, Testing mode-coupling theory for a supercooled binary Lennard–Jones mixture I: the van hove correlation function. *Phys. Rev. E* **51**(5), 4626 (1995)
7. T.A. Weber, F.H. Stillinger, Local order and structural transitions in amorphous metal–metalloid alloys. *Phys. Rev. B* **31**(4), 1954 (1985)
8. M. Wakada, T. Ichitsubo, Atomistic study of liquid fragility and spatial heterogeneity of glassy solids in model binary alloys. *NPG Asia Mater.* **15**, 46 (2023)
9. H. Tong, H. Tanaka, Role of attractive interactions in structure ordering and dynamics of glass-forming liquids. *Phys. Rev. Lett.* **124**(22), 225501 (2020)
10. J. Chatteraj, M.P. Ciamarra, Role of attractive forces in the relaxation dynamics of supercooled liquids. *Phys. Rev. Lett.* **124**(2), 028001 (2020)
11. E. Attia, J.C. Dyre, U.R. Pedersen, Comparing four hard-sphere approximations for the low-temperature WCA melting line. *J. Chem. Phys.* **157**(3), 034502 (2022)
12. R. Brüning, D.A. St-Onge, S. Patterson, W. Kob, Glass transitions in one-, two-, three-, and four-dimensional binary Lennard–Jones systems. *J. Phys. Condens. Matter* **21**(3), 035117 (2008)
13. S. Toxvaerd, U.R. Pedersen, T.B. Schröder, J.C. Dyre, Stability of supercooled binary liquid mixtures. *J. Chem. Phys.* **130**(22), 224501 (2009)
14. U.R. Pedersen, T.B. Schröder, J.C. Dyre, Phase diagram of Kob–Andersen-type binary Lennard–Jones mixtures. *Phys. Rev. Lett.* **120**(16), 165501 (2018)
15. S. Sastry, The relationship between fragility, configurational entropy and the potential energy landscape of glass-forming liquids. *Nature* **409**(6817), 164–167 (2001)
16. J. Wittmer, H. Xu, P. Polińska, F. Weysser, J. Baschnagel, Shear modulus of simulated glass-forming model systems: effects of boundary condition, temperature, and sampling time. *J. Chem. Phys.* **138**(12), 12A533 (2013)
17. J.D. Weeks, D. Chandler, H.C. Andersen, Role of repulsive forces in determining the equilibrium structure of simple liquids. *J. Chem. Phys.* **54**(12), 5237–5247 (1971)
18. L. Berthier, G. Tarjus, Nonperturbative effect of attractive forces in viscous liquids. *Phys. Rev. Lett.* **103**(17), 170601 (2009)
19. J.E. Lennard-Jones, Cohesion. *Proc. Phys. Soc.* **43**(5), 461–482 (1931)
20. E. Helfand, Transport coefficients from dissipation in a canonical ensemble. *Phys. Rev.* **119**(1), 1 (1960)
21. R.K. Murarka, B. Bagchi, Diffusion and viscosity in a supercooled polydisperse system. *Phys. Rev. E* **67**(5), 051504 (2003)
22. O.A. Moulton, Y. Zhang, I.N. Tsimpanogiannis, I.G. Economou, E.J. Maginn, System-size corrections for self-diffusion coefficients calculated from molecular dynamics simulations: the case of CO₂, *n*-alkanes, and poly(ethylene glycol) dimethyl ethers. *J. Chem. Phys.* **145**(7), 074109 (2016)
23. K.-S. Kim, M.H. Han, C. Kim, Z. Li, G.E. Karniadakis, E.K. Lee, Nature of intrinsic uncertainties in equilibrium molecular dynamics estimation of shear viscosity for simple and complex fluids. *J. Chem. Phys.* **149**(4), 044510 (2018)
24. A.P. Thompson, H.M. Aktulga, R. Berger, D.S. Bolintineanu, W.M. Brown, P.S. Crozier, P.J. Veld, A. Kohlmeyer, S.G. Moore, T.D. Nguyen, R. Shan, M.J. Stevens, J. Tranchida, C. Trott, S.J. Plimpton, LAMMPS—a flexible simulation tool for particle-based materials modeling at the atomic, meso, and continuum scales. *Comput. Phys. Commun.* **271**, 108171 (2022)
25. MathWorks: MATLAB, R2023a. <https://www.mathworks.com>
26. J. Chun, B. Lee, Atomistic calculations of mechanical properties of Ni-Ti-C metallic glass systems. *J. Mech. Sci. Technol.* **27**, 775–781 (2013)

Publisher's Note Springer Nature remains neutral with regard to jurisdictional claims in published maps and institutional affiliations.

Springer Nature or its licensor (e.g. a society or other partner) holds exclusive rights to this article under a publishing agreement with the author(s) or other rightsholder(s); author self-archiving of the accepted manuscript version of this article is solely governed by the terms of such publishing agreement and applicable law.